

SAR Oil Palm Plantation Mapping in Batu Pahat with X, C, L bands for Change Detection

James Yong Peng Ang¹, Zhi Qing Ng¹

¹ST Engineering Geo-Insights Pte Ltd, 6 Ang Mo Kio Electronics Park Road #06-03 Singapore –
(james.angyp,zhiqing.ng)@stengg.com

Keywords: Oil Palm Plantation, Synthetic Aperture Radar, Feature Pyramid Network, Change Detection.

Abstract

Oil palms have large economic value and are grown extensively across Southeast Asia. However, growth of the oil palm industry comes at the expense of the environment as forests are cleared to grow oil palms. Oil palm plantations need to be monitored to balance economic growth and environmental sustainability. Synthetic Aperture Radar (SAR) imagery allows for the cost-effective and frequent mapping of the extent of oil palm plantations over large areas. This paper aims to develop an oil palm plantation mapping model using X, C and L band SAR and compare their relative performance. The models are developed with the Feature Pyramid Network based on annotations acquired over Batu Pahat, Malaysia. X-band has the best Dice Score of 0.9 for oil palm plantations and the highest overall accuracy of 81.78%. Repeat pass satellite images captured 6 months later were then inferred with the 3 models to identify changes to the land cover. X-band also has the best accuracy in change detection as it has the best land cover classification performance overall. The plantation maps add semantic meaning to the land cover changes. This paper successfully developed a model that can generate frequently updated and detailed oil palm plantation maps, which can be used to detect changes in the oil palm plantation extent promptly.

1. Introduction

Oil palms have large economic value and are commonly grown across Southeast Asia. They produce the most oil per crop compared to other oil crops and have the largest demand among all vegetable oils worldwide. However, the growth of the oil palm industry threatens biodiversity and the environment as forests are cleared to make way for oil palm plantations (Chong et al., 2017). Therefore, it is important to generate accurate oil palm plantation maps for the relevant stakeholders to track the rate of expansion of oil palm plantations, evaluate its impact on the environment and develop land use policies that balance economic growth and environmental sustainability (Zeng et al., 2022).

Satellite imaging allows for the cost-effective mapping of oil palm plantations over large areas. Both electro-optical (EO) and synthetic aperture radar (SAR) satellites can generate large-scale oil palm plantation maps. SAR satellites have a clear advantage over EO as they are active sensors and thus able to operate regardless of cloud cover and daylight. This is especially important in the tropics where cloud covers are frequent. Hence, SAR is better able to meet the frequency of update required. SAR operates at different wavelengths, such as the X-band (3cm wavelength), C-band (5.6cm wavelength) and L-band (21cm wavelength). Each wavelength penetrates vegetation canopy differently and thus each band is suitable for classifying different land cover classes. At longer wavelengths (L-band), SAR can penetrate vegetation canopy to a larger extent (Tsyganskaya et al., 2018). Studies found that L-band backscatter has higher sensitivity for vegetation with higher biomass while X-band is more suited for low biomass conditions (Wohlfart et al., 2018). L band is reported to be best for mapping forested vegetation and oil palms due to its largest penetration depth to detect vegetation subcanopy (Chong et al., 2017). This paper will compare the relative performance of the X, C and L bands for plantation mapping and evaluate their suitability for monitoring changes to the land cover with respect to oil palm plantations.

This paper aims to develop an oil palm plantation mapping technique based on annotations acquired over oil palm plantations in Batu Pahat. Other land cover types in the area will also be included in the training, such as other vegetation and barren land. Oil palm plantation maps will be developed using each of the X, C and L bands and their respective performance compared. A state-of-the-art CNN architecture, the Feature Pyramid Network (FPN), will be used to develop the plantation maps. The model will then be applied to detect changes in the land cover with respect to oil palm plantations in Batu Pahat. The land cover labels provide semantic information to help the relevant stakeholders to interpret the change and follow up with necessary actions.

2. Related Work

There have been ongoing research efforts to study oil palm plantation mapping using satellite images. Most researchers combine both EO and SAR images to map the land cover of the area of interest, including oil palm plantations. (Xu et al., 2021) trained a Random Forest model on both Landsat 8 and Sentinel 1 images to classify mature, young oil palm plantations and bare land in Riau province, Indonesia. (Monsalve-Tellez et al., 2022) also used Random Forest to develop a model to classify oil palm, waterbodies, grassland, forest, bare soil and low vegetation using Sentinel 1 and 2 over Colombia. (Descals et al., 2020) developed a DeepLabV3+ model to segment the 7 tropical regions of the world into industrial, smallholder oil palm plantations and others based on Sentinel 1 and Sentinel 2 imagery. Although fusing data across different imaging sensors improves model performance most of the time (Zeng et al., 2022), it also increases the amount of data required and thus incurs additional costs. Hence, it is important to determine the best performing SAR imaging band for oil palm plantation classification and change detection before merging data from different bands.

There has been limited studies comparing the performance of different SAR imaging bands for oil palm plantation mapping. (Busquier et al., 2022) postulated that the best band depends on

the size of scattering target with respect to the magnitude of the operating wavelength and penetration depth of the imaging band. He compared the performance of TanDEM-X (X-band), Sentinel-1 (C-band) and ALOS2-PALSAR (L-band) for land cover and crop classification using Random Forest. For land cover classification, L-band gave the best overall performance with overall accuracy at 81%. The best performing classes for L-band were cultivated land, olive grove and fruit trees. However, for crop classification, C-band gave the best overall performance with an overall accuracy of 78%. This suggests that the best performing bands is dependent on the classes considered. The researchers considered a wide range of classes for land cover classification (Pirotti et al., 2023), such as forests, rice fields, waterbodies, residential areas etc, but not oil palm plantations. Specific to oil palm plantations, (Zeng et al., 2022) compared the performance of Sentinel 1, ALOS2-PALSAR, Sentinel-2, Landsat-8 and its combinations. Sentinel 1 had a better accuracy for oil palm classification than ALOS2-PALSAR and, overall. This paper will also compare the relative performance of X, C and L bands and go a step further to evaluate their performance for change detection with respect to oil palm plantations.

3. Methodology

Manual annotations were conducted by referencing high resolution EO satellite imagery and used to train a FPN model for X, C and L-band SAR images respectively. Performance of each model on a hold-out validation dataset was compared. The model was then used to detect changes to the land cover in Batu Pahat over a span of about 6 months.

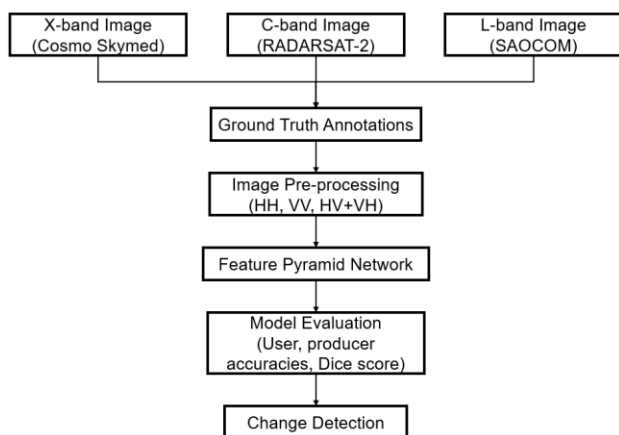


Figure 1: Methodology Overview

3.1 Study Area

The study area for this paper is at Batu Pahat, Malaysia. Batu Pahat is in the state of Johor, with most of the area covered by plantations. It is also a rapidly developing district and thus, much changes to the land cover would be expected (Hsin, 2007). Therefore, Batu Pahat is a suitable site for oil palm classification and change detection.



Figure 2: Batu Pahat Location on the left and Land Cover Map from European Space Agency. Area of Interest Marked in Purple

3.2 Data Acquisition

Cosmo SkyMed Second Generation (CSG) (X-band), RADARSAT-2 (RS2) (C-band) and Satellite for Earth Observation with Microwave Radar (SAOCOM) (L band) images were acquired over Batu Pahat in February 2022. More details about the image acquisition are described in Table 1. All acquired images were fully polarised (HH, HV, VH, VV), taken in stripmap mode and right-looking.

Manual annotations were derived based on high resolution Pleiades Neo EO satellite imagery captured on 10 February 2022. The land cover classes considered in this paper are as listed in Table 2 below.

	CSG	RS2	SAOCOM
Acquisition Date	16/02/2022	19/02/2022	26/02/2022
Wavelength (cm)	3.1	5.5	24.2
Orbit Direction	Ascending	Descending	Descending
Incidence Angle	23.9°	39.1°	26.2°
Pixel Spacing (m)	1.5	2.5	2.5

Table 1: SAR Image Acquisition over Batu Pahat

Class	Description
Plantation (PLT)	Oil palm plantations, vegetation grown in regular patterns
Other Vegetation (VEG)	All other types of vegetation that are not oil palm plantations, such as forests, grasslands, mangroves and small bushes
Cropland (CRL)	Young oil palm plantations, other cultivated land with no obvious tree crowns
Barren (BRN)	Exposed soil, clearings, no vegetation
Others (OTH)	Other land cover types such as buildings, roads and waterbodies

Table 2: Land Cover Classes for Oil Palm Plantation Mapping

3.3 Image Pre-processing

The SAR images were acquired in the Level 1 Single Look Complex (SLC) form. The images then undergo geocoding and were converted to sigma nought dB. Lexicographic decomposition was adopted, and all 4 polarisation modes were stacked to produce a 3-channel image, with the channels being HH, VV and HV+VH.

The backscatter distributions of the SAR images were calculated and compared to evaluate the separability of the classes proposed. This paper will compare the backscatter distribution of plantations with other vegetation, cropland and barren which are the classes of interest. Tables 3 to 5 list the lower quartile, median and upper quartile for these classes. The Plantation class generally has a larger median backscatter

coefficient compared to the other classes, except for the HV+VH channel where the backscatter coefficient of plantations is lower than that of other vegetation and cropland. SAOCOM HH channel has the largest difference of 1.39dB between the backscatter coefficients of plantations and other vegetation. SAOCOM HV+VH channel has the largest difference of 1.69 dB between the backscatter coefficients of plantations and cropland. Backscatter coefficient of barren land is generally lower than plantation, other vegetation and cropland as the backscatter of bare land is mostly made up of surface scattering alone. Hence, barren land is most separable from plantations as evident in their backscatter return distributions. SAOCOM HV+VH channel gives the largest difference of 4.15 dB between the backscatter coefficients of plantation and barren land. SAOCOM HV+VH channel also produces the largest difference of 4.43 dB between the backscatter coefficients of other vegetation and barren land. Thus, L-band has the best separability for the classes of interest, especially for HV+VH polarisation. Nonetheless, backscatter difference is not the only factor determining model performance, as FPN also considers the texture and backscatter of nearby pixels before generating a label.

	Lower Quartile	Median	Upper Quartile
HH Polarisation (dB)			
PLT	-17.25	-13.42	-9.98
VEG	-18.89	-14.67	-10.76
CRL	-17.86	-14.07	-10.63
BRN	-20.56	-16.12	-12.06
VV Polarisation (dB)			
PLT	-18.3	-14.43	-10.95
VEG	-19.95	-15.71	-11.77
CRL	-18.98	-15.16	-11.7
BRN	-21.67	-17.35	-13.36
HV+VH Polarisation (dB)			
PLT	-19.69	-16.46	-13.36
VEG	-20.17	-16.44	-12.82
CRL	-19.72	-16.41	-13.23
BRN	-23.37	-19.33	-15.39

Table 3: Lower Quartile, Median, Upper Quartile of Backscatter for Plantation, Other Vegetation, Cropland and Barren for X-band (CSG)

	Lower Quartile	Median	Upper Quartile
HH Polarisation (dB)			
PLT	-15.43	-11.64	-8.3
VEG	-16.76	-12.65	-8.94
CRL	-15.9	-12.12	-8.78
BRN	-18.91	-14.34	-10.23
VV Polarisation (dB)			
PLT	-15.54	-11.73	-8.38
VEG	-17	-12.89	-9.18
CRL	-16.36	-12.55	-9.16
BRN	-19.34	-14.95	-10.97
HV+VH Polarisation (dB)			
PLT	-17.02	-13.45	-10.21
VEG	-17.05	-13.16	-9.56
CRL	-16.76	-13.14	-9.84
BRN	-20.68	-16.4	-12.37

Table 4: Lower Quartile, Median, Upper Quartile of Backscatter for Plantation, Other Vegetation, Cropland and Barren for C-band (RS2)

	Lower Quartile	Median	Upper Quartile
HH Polarisation (dB)			
PLT	-13.87	-10.36	-7.25
VEG	-15.64	-11.75	-8.15
CRL	-15.59	-11.92	-8.56
BRN	-17.7	-13.31	-9.15
VV Polarisation (dB)			
PLT	-16.44	-12.94	-9.83
VEG	-17.14	-13.27	-9.62
CRL	-17.28	-13.62	-10.24
BRN	-18.86	-14.61	-10.58
HV+VH Polarisation (dB)			
PLT	-16.67	-13.31	-10.28
VEG	-16.92	-13.03	-9.35
CRL	-18.5	-15	-11.72
BRN	-21.89	-17.46	-13.23

Table 5: Lower Quartile, Median, Upper Quartile of Backscatter for Plantation, Other Vegetation, Cropland and Barren for L-band (SAOCOM)

3.4 Model

FPN consists of a bottom up and a top-down pathway as illustrated in Figure 3. The bottom-up pathway computes feature maps at several scales where the scale reduces by 2 at the next stage. The top-down pathway then upsamples these feature maps by 2 and merge with the corresponding feature map of the same scale created in the bottom-up pathway. This pyramidal architecture allows objects to be detected at different scales. FPN can be modified to produce segmentation maps by using fully convolutional layers (Lin et al., 2017).

ResNeXt with squeeze and excite blocks (SE-ResNeXt) is selected as the backbone convolutional architecture to generate the feature maps. ResNeXt builds upon Residual Neural Networks (ResNet) by introducing a new dimension – the number of parallel transformations in a group with the same topology, also known as cardinality. This allows the model to capture different features while maintaining the model complexity (Xie et al., 2017). Squeeze and excite block is a module added to ResNeXt for feature calibration across channels. The block first applies average pooling across channels to extract channel statistics. This is followed by a gate with sigmoid activation function to learn the non-linear dependencies across channels (Hu et al., 2018).

Each SAR image (HH, VV, HV+VH) was split into tiles of 512 by 512 pixels and 3 channels. Each task has a corresponding mask with a label per pixel. The tile-mask pairs were used to train the FPN model. The FPN model outputs a label for each pixel in the tile, which can then be stitched together to produce an oil palm plantation map for each SAR image. The FPN model was trained on a machine equipped with NVIDIA GeForce RTX 3090 GPU with 24 GB RAM.

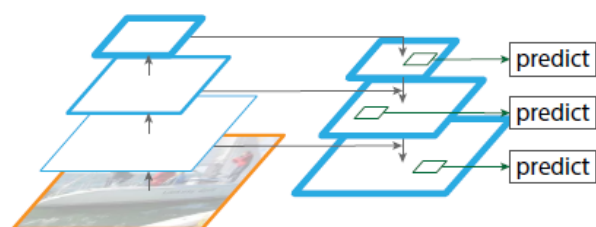


Figure 3: FPN Architecture (Lin et al., 2017)

4. Results

4.1 Performance Assessment

The performance of the respective SAR imaging bands will be assessed with producer and user accuracy and Dice score for each class and the overall accuracy and Kappa Coefficient. The producer accuracy measures the proportion of pixels of each class that are correctly classified whereas the user accuracy computes the probability that a pixel identified as class Y is truly from class Y (Story and Congalton, 1986). Dice score combines both producer and user accuracy (Müller et al., 2022). Kappa coefficient measures the degree of agreement between the predicted labels and the ground truth (Rwanga et al., 2017). Overall accuracy measures the percentage of pixels correctly classified.

Other than high producer and user accuracy for plantation and cropland, high producer and user accuracies for other vegetation and barren land are also desirable as other vegetation could be cleared for palm plantation. Therefore, the best model should have high dice scores for plantation, cropland, other vegetation and barren land to ensure the best accuracy and lowest false alarm rates possible.

4.2 Model Performance on Study Area

The confusion matrices of the X, C and L band models are provided in Table 6 to Table 8 below. The X-band model has the best overall performance as evident in its largest overall accuracy of 81.78% and Kappa Coefficient of 0.73. X-band has the best producer (88.07%), user (92.85%) accuracy and dice score (0.9) for plantations. This performance is a significant improvement from the producer (88%) and user (74%) accuracies reported by (Zeng et al., 2022) for oil palms in Muda River Basin, Malaysia using Random Forest on Google Earth Engine. (Monsalve-Tellez et al., 2022) achieved a better producer and user accuracy of both 94.29% for oil palms over Columbia, also using Random Forest on Google Earth Engine. (Monsalve-Tellez et al., 2022) further included various SAR indices for classification, which could have contributed to the better performance. Further research can be conducted to include SAR indices for oil palm plantation mapping and change detection.

X-band also has the best producer (78.7%), user (80.51%) and Dice score (0.8) for other vegetation. The L-band model had the largest producer accuracy (75.03%) while the X-band model had the largest user accuracy (67.03%) for cropland. C and L-band models had a significantly lower user accuracy of 29.42% and 30.02% respectively for cropland. This is due to an over-classification of other vegetation as cropland – 10.93% for C-band and 11.32% for L-band. The X-band model has the largest producer accuracy (60.36%) while L-band model has the largest user accuracy (64.7%) for the barren class. All 3 bands have Dice scores at 0.56. Overall, X-band is most suitable for plantation mapping due to its better classification performance for plantation, other vegetation and cropland.

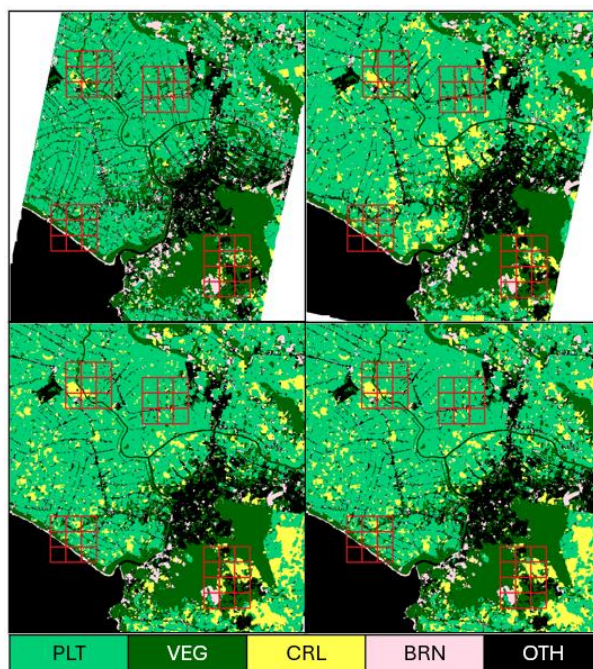


Figure 4: Inference Result for X (Top Left), C (Top Right) and L (Bottom Left) bands With Ground Truth (Bottom Right) for Reference. Hold-out validation set marked in red

	PLT	VEG	CRL	BRN	OTH
PLT	88.07	6.02	0.92	1.32	3.67
VEG	6.81	78.70	2.09	4.91	7.49
CRL	13.17	21.50	58.41	4.59	2.33
BRN	4.91	16.27	3.08	60.36	15.38
OTH	2.65	8.77	0.23	5.66	82.69
Overall Accuracy: 81.78% Kappa Coefficient: 0.73					

Table 6: X-band (CSG) Confusion Matrix (%)

	PLT	VEG	CRL	BRN	OTH
PLT	84.90	5.32	6.16	0.41	3.21
VEG	12.04	66.71	10.93	2.78	7.54
CRL	16.68	15.73	64.78	2.15	0.66
BRN	9.59	15.76	7.30	50.08	17.28
OTH	7.01	11.27	1.70	3.44	76.58
Overall Accuracy: 75.62% Kappa Coefficient: 0.64					

Table 7: C-band (RS2) Confusion Matrix (%)

	PLT	VEG	CRL	BRN	OTH
PLT	85.98	4.51	7.25	0.39	1.87
VEG	14.60	65.53	11.32	2.66	5.89
CRL	13.55	8.84	75.03	1.24	1.35
BRN	10.52	17.84	9.13	49.47	13.04
OTH	9.13	14.15	2.66	3.19	70.86
Overall Accuracy: 75.49% Kappa Coefficient: 0.64					

Table 8: L-band (SAOCOM) Confusion Matrix (%)

	PLT	VEG	CRL	BRN	OTH
Producer Accuracy (%)					
X	88.07	78.70	58.41	60.36	82.69
C	84.90	66.71	64.78	50.08	76.58
L	85.98	65.53	75.03	49.47	70.86
User Accuracy (%)					
X	92.85	80.51	67.03	51.55	67.51
C	87.53	78.70	29.42	63.12	66.62
L	85.92	79.09	30.02	64.70	71.96
Dice Score					
X	0.90	0.80	0.62	0.56	0.74
C	0.86	0.72	0.40	0.56	0.71
L	0.86	0.72	0.43	0.56	0.71

Table 9: Producer, User Accuracy and Dice Scores for X, C and L bands

4.3 Change Detection

Changes to the oil palm plantation map indicate possible changes to the land cover that could be of interest to the relevant stakeholders. Repeat pass SAR images were acquired about 6 months later as detailed in Table 10. Oil palm plantation maps were then generated through inference with the model trained in Section 3.4. Figure 5 to Figure 7 indicate some of the changes detected by the plantation maps for X, C and L bands respectively. These examples cover 3 possible scenarios – plantation clearing, growth of young plantations/cropland and forest clearing.

X band gives the best performance for change detection due to its best accuracy for plantation, other vegetation, cropland and overall. The C-band model misclassified barren as plantation in Figure 6 and Figure 7. This could be attributed to C-band's lower producer accuracy for barren class, where 9.59% of barren pixels were misclassified as plantation. The L-band model misclassified cropland as plantation in Figure 6. This is a common problem among the X, C and L bands generally. Across the entire validation set, the X-band model misclassified 13.17% of cropland as plantation, for C-band 16.68% and for L-band 13.55%.

Land cover labels also provided useful semantic information about the changes that occurred. For example, Figure 7 illustrates an example of a forest clearing. The area of forests cleared can be measured by the change in area of the other vegetation class in the inference result. The same area can be captured by satellite imagery and inferred several months later to determine if the forests were cleared for oil palm plantations. This paper has demonstrated how the oil palm plantation maps can be utilised to understand and measure the changes to the land cover over a large area.

	CSG	RS2	SAOCOM
Acquisition Date	11/08/2022	06/08/2022	20/07/2022
Wavelength (cm)	3.1	5.5	24.2
Orbit Direction	Ascending	Descending	Descending
Incidence Angle	23.9°	39.1°	26.2°
Pixel Spacing (m)	1.5	2.5	2.5

Table 10: SAR Image Acquisition over Batu Pahat for Change Detection

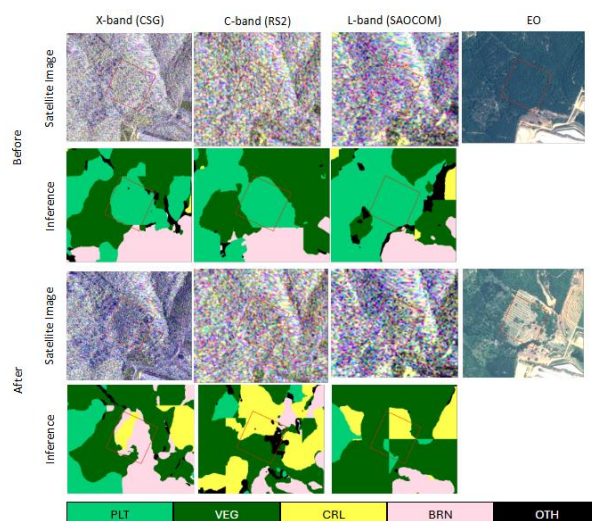


Figure 5: Plantation Clearing Detection with X, C and L bands

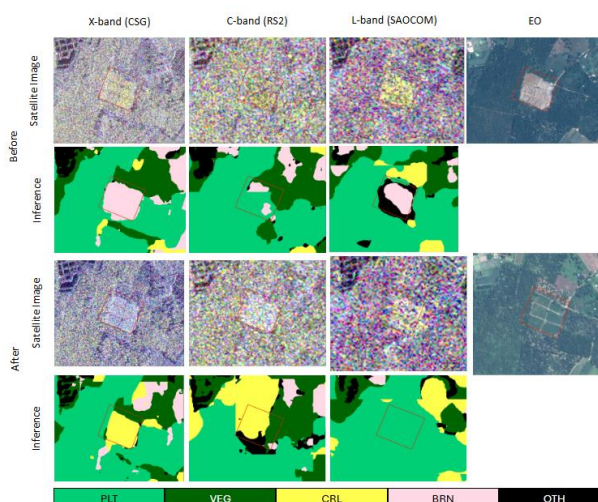


Figure 6: Cropland Growth Detection with X, C and L bands

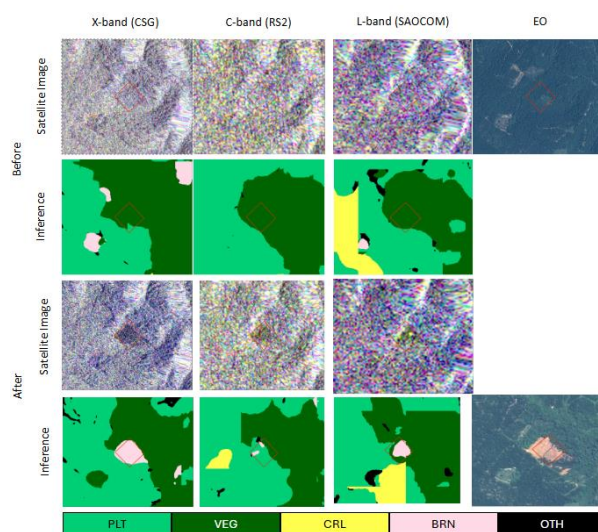


Figure 7: Forest Clearing Detection with X, C and L bands

5. Discussion

The developed model successfully identifies the mature and young oil palm plantations in Batu Pahat, with minimal misclassifications with other classes such as other vegetation. All 3 bands achieve a high dice score of at least 0.86 for the plantation class, with X-band (CSG) having the highest producer (88.07%) and user (92.85%) accuracy. Section 3.3 has earlier established that L-band has the best separability for plantation against other vegetation, barren land and cropland based on its backscatter distribution. However, the results indicated that X-band performed the best among the 3 imaging bands, which could be attributed to how C and L bands significantly confuses mature plantations (Plantation class) with young plantations (Cropland class). 6.16% of plantations were wrongly classified as cropland for C-band and 7.25% for L band. As oil palms age, their heights increase, frond lengths increase, and the number of leaves and branches increases (Carolita et al., 2021). X-band could be better able to detect the increase in number of leaves as the width of the oil palm leaflets is closer to X-band's wavelength. Hence, X-band is better able to separate mature and young oil palm plantations.

X-band also has the best resolution and thus gives the best performance for classes that are more sensitive to texture differences. For classes such as barren with fewer texture variations, all 3 bands have similar performance as evident from the same Dice score.

X-band also demonstrated the best performance to detect changes to the land cover with respect to oil palm plantations. This is a direct result of X-band's better performance in land cover classification shown in Section 4.2.

With X-band established as the best performing SAR imaging band, a new oil palm plantation model can be trained after fusing X-band and high resolution EO imagery. The new data source should also match the high resolution of X-band SAR as resolution has been determined to be an important factor in land cover classification. More manual annotations can also be acquired over oil palm plantations in other parts of Malaysia to produce an accurate oil palm plantation mapping model that can be deployed across the country.

6. Conclusion

An oil palm plantation mapping model was developed for Batu Pahat using Feature Pyramid Network for X, C and L bands respectively. The model has achieved high accuracy for plantation mapping, achieving a Dice score of around 0.86 to 0.9. While L-band has the best separability for its backscatter, X-band achieved the best performance for both plantation and cropland due to the least confusion between mature and young oil palm plantations (plantation versus cropland). X-band's good performance could be attributed to its finer resolution and how its wavelength is close to the width of the oil palm leaflets. The plantation mapping model is also applied to infer repeat pass satellite images to detect changes to the land cover. X-band also detects changes most accurately due to its best land cover classification performance. The performance of the oil palm plantation mapping model can be further enhanced by fusing high resolution EO data and training with more annotations over other oil palm plantations in Malaysia.

References

Busquier, M., Lopez-Sanchez, J. M., Ticconi, F., Flourey, N.,

2022. Combination of time series of L-, C-, and X-band SAR images for land cover and crop classification. *IEEE Journal of Selected Topics in Applied Earth Observations and Remote Sensing*, 15, 8266–8286.

Carolita, I., Rosid, M., Ibrahim, A., Dirgahayu, D., Noviar, H., Supriatna, J., 2021. Potential of palar scansar data for oil palm plantation in growth monitoring and mapping. *IOP Conference Series: Earth and Environmental Science*, 739 (1), IOP Publishing, 012091.

Chong, K. L., Kanniah, K. D., Pohl, C., Tan, K. P., 2017. A review of remote sensing applications for oil palm studies. *Geospatial Information Science*, 20(2), 184–200.

Descals, A., Wich, S., Meijaard, E., Gaveau, D. L., Peedell, S., Szantoi, Z., 2020. High-resolution global map of smallholder and industrial closed-canopy oil palm plantations. *Earth System Science Data Discussions*, 2020, 1–22.

Fawzy, M., Szabó, G., Barsi, A., 2023. A Shallow Neural Network Model for Urban Land Cover Classification Using VHR Satellite Image Features. *ISPRS Annals of the Photogrammetry, Remote Sensing and Spatial Information Sciences*, 10, 57–64.

Hsin, L., 2007. Water quality study of Sungai Batu Pahat. Universiti Teknologi Malaysia.

Hu, J., Shen, L., Sun, G., 2018. Squeeze-and-excitation networks. *Proceedings of the IEEE conference on computer vision and pattern recognition*, 7132–7141.

Iakubovskii, P., 2019. Segmentation models. <https://github.com/qubvel/segmentationmodels>.

Lin, T.-Y., Dollár, P., Girshick, R., He, K., Hariharan, B., Belongie, S., 2017. Feature pyramid networks for object detection. *Proceedings of the IEEE conference on computer vision and pattern recognition*, 2117–2125.

Monsalve-Tellez, J. M., Torres-León, J. L., Garcés-Gómez, Y. A., 2022. Evaluation of SAR and optical image fusion methods in oil palm crop cover classification using the random forest algorithm. *Agriculture*, 12(7), 955.

Müller, D., Soto-Rey, I., Kramer, F., 2022. Towards a guideline for evaluation metrics in medical image segmentation. *BMC Research Notes*, 15(1), 210.

Pirotti, F., Adedipe, O., Leblon, B., 2023. Sentinel-1 Response to Canopy Moisture in Mediterranean Forests before and after Fire Events. *Remote Sensing* 15, 823.

Rwanga, S. S., Ndambuki, J. M. et al., 2017. Accuracy assessment of land use/land cover classification using remote sensing and GIS. *International Journal of Geosciences*, 8(04), 611.

Shevade, V. S., Loboda, T. V., 2019. Oil palm plantations in Peninsular Malaysia: Determinants and constraints on expansion. *PLoS One*, 14(2), e0210628.

Story, M., Congalton, R. G., 1986. Accuracy assessment: a user's perspective. *Photogrammetric Engineering and remote sensing*, 52(3), 397–399.

Tsyganskaya, V., Martinis, S., Marzahn, P., Ludwig, R., 2018. SAR-based detection of flooded vegetation—a review of characteristics and approaches. *International journal of remote sensing*, 39(8), 2255–2293.

Wohlfart, C., Winkler, K., Wendleder, A., Roth, A., 2018. TerraSAR-X and wetlands: A review. *Remote Sensing*, 10(6), 916.

Xie, S., Girshick, R., Dollár, P., Tu, Z., He, K., 2017. Aggregated residual transformations for deep neural networks. *Proceedings of the IEEE conference on computer vision and pattern recognition*, 1492–1500.

Xu, K., Qian, J., Hu, Z., Duan, Z., Chen, C., Liu, J., Sun, J., Wei, S., Xing, X., 2021. A new machine learning approach in detecting the oil palm plantations using remote sensing data. *Remote Sensing*, 13(2), 236.

Zanaga, D., Van De Kerchove, R., Daems, D., De Keersmaecker, W., Brockmann, C., Kirches, G., Wevers, J., Cartus, O., Santoro, M., Fritz, S. et al., 2022. ESA WorldCover 10 m 2021 v200.

Zeng, J., Tan, M. L., Tew, Y. L., Zhang, F., Wang, T., Samat, N., Tangang, F., Yusop, Z., 2022. Optimization of Open-Access Optical and Radar Satellite Data in Google Earth Engine for Oil Palm Mapping in the Muda River Basin, Malaysia. *Agriculture*, 12(9), 1435.